Pergamon

Int. Comm. Heat Mass Transfer, Vol. 30, No. 3, pp. 435-444, 2003

0735–1933/03/$–see front matter

Available online at www.sciencedirect.com

SCIENCE DIRECT®

PII: S0735-1933(03)00061-7

NUMERICAL INVESTIGATION OF SHROUDED FIN ARRAY UNDER COMBINED FREE AND FORCED CONVECTION

A. Al-Sarkhi, E. Abu-Nada, B. A. Akash, J. O. Jaber
Department of Mechanical Engineering
Hashemite University
Zarqa, 13115, JORDAN
E-mail: alsarkh@hu.edu.jo

(Communicated by J.P. Hartnett and W.J. Minkowycz)

ABSTRACT

The influence of combined free and forced convection in a vertical shrouded fin is considered in this paper. Nusselt number, Nu, and friction factor multiplied by Reynolds number, fRe, are functions of the buoyancy force which is associated strongly with the geometry of the shrouded fin (the clearance above the fin tip and the spacing between adjacent fins). Nu and fRe increase nonlinearly with increasing the clearance above the fin tip. The results obtained from this work can be helpful in the characteristics evaluation of shrouded fins.

Introduction

Fins are commonly used in many applications when enhancement in the process of heating up or cooling down is required. The compactness and spatial geometry of fins is very important for best design. Several studies have been conducted on different shapes of fins [1-5]. An experimental work was conducted to study steady state heat transfer from pin-fin array [6]. Sara et al. [7] studied the heat transfer enhancement in a channel with rectangular block fins. Watel et al. [8] investigated experimentally the influence of fin spacing and rotational speed on the convective heat exchanges from a rotating finned tube. Natural convection in a periodically finned vertical channel was investigated experimentally by Daloglu and Ayhan [9].

The Shrouded fin is characterized by a flow in a channel as shown in Figure 1. The amount of heat transfer depends on the flow distribution around the fin, which depends on the dimensions of the fin clearance and the distance between the arrays of fins. The combined free and forced convection, in a fin oriented vertically, will be considered in this paper. The buoyancy force has an influence on the flow distribution around the fin. The effect of buoyancy was addressed in a horizontal shrouded fin by Acharya and Patankar [10]. The vertical flow in shrouded fin studied by Zhang and Patankar [11] for limited cases. In this paper wider range of Rayleigh number, Ra, and spatial dimensions of the fin will be considered. Also different numerical technique with finer grid will be used.

At a certain situation most of the fluid flows in the clearance above the fin tip which leads to less enhancement in heat transfer from the fin. In another scenario most of the fluid flows in the spacing between the fins, which enhances the heat transfer. The velocity and the temperature distribution are functions of Rayleigh number and geometry of the spacing, and clearance of the shrouded fin.

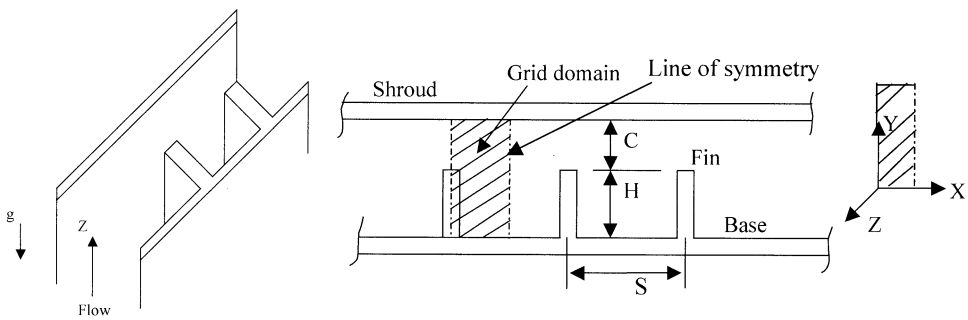

FIG. 1
Schematic diagram of the shrouded fin array

Governing Equations and Methodology

The flow field in the shrouded fin under investigation is assumed to be laminar and fully developed, with constant heat flux per unit streamwise length. Fluid properties are constant except for the buoyancy term. The fin thickness is negligible. The base and fins are made of a material of high thermal conductivity to ensure having a uniform temperature in any cross section. The shroud is assumed to have an adiabatic boundary condition. The flow is assumed to be heated up-flow. Taking all the above assumptions into consideration and follow the same procedure described in ref. [11], the governing equations of momentum and energy in a fully developed region can be written as:

$$\frac{\partial}{\partial x}\left(\mu\frac{\partial w}{\partial x}\right)+\frac{\partial}{\partial y}\left(\mu\frac{\partial w}{\partial y}\right)-\frac{dp}{dz}+\rho g=0 \tag{1}$$

$$\rho c_p\, w\frac{\partial T}{\partial z}=\frac{\partial}{\partial x}\left(k\frac{\partial T}{\partial x}\right)+\frac{\partial}{\partial y}\left(k\frac{\partial T}{\partial y}\right) \tag{2}$$

For constant heat flux,

$$\frac{\partial T}{\partial z}=\frac{\partial T_w}{\partial z}=\frac{\partial T_b}{\partial z}=\frac{Q}{\dot{m}c_p} \tag{3}$$

$$\dot{m}=\rho\overline{w}V(h+c)\frac{b}{2}=\rho\iint V dxdy \tag{4}$$

The effect of natural convection is introduced through a Boussinesq approximation:

$$\rho=\rho_w\left(1-\beta(T-T_w)\right) \tag{5}$$

Normalizing the coordinates, axial velocity and the temperature as:

$$\mathrm{X}=\mathrm{x/H},\ \mathrm{Y}=\mathrm{y/H},\quad \Omega=-\frac{w\mu}{H^2\left((dp/dz)+\rho_w g\right)}$$

$$Ra=\frac{\rho_w\beta g(dT_b/dz)}{\alpha\mu},\quad \theta=\frac{T_w-T}{Q/k}$$

Normalizing the governing equation using equations (3), (4) and (5)

$$\frac{\partial^2\Omega}{\partial X^2}+\frac{\partial^2\Omega}{\partial Y^2}+Ra\cdot\theta\cdot\Omega^*+1=0 \tag{6}$$

$$\frac{\partial^2\theta}{\partial X^2}+\frac{\partial^2\theta}{\partial Y^2}-\frac{\Omega}{\Omega^*}=0 \tag{7}$$

where $\Omega^*=\iint\Omega dXdY$ is evaluated over the grid domain under consideration

Introducing new variable $\phi=\theta\cdot\Omega^*$ the final forms of the governing equations become

$$\frac{\partial^2\Omega}{\partial X^2}+\frac{\partial^2\Omega}{\partial Y^2}+Ra\cdot\phi+1=0 \tag{8}$$

$$\frac{\partial^2\phi}{\partial X^2}+\frac{\partial^2\phi}{\partial Y^2}-\Omega=0 \tag{9}$$

The boundary conditions for the above governing equations are:

Base and fin:	$\Omega=0,$	$\phi=0$
Shroud:	$\Omega=0,$	$\partial\phi/\partial\mathrm{Y}=0$
Symmetry planes:	$\partial\Omega/\partial\mathrm{X}=0,$	$\partial\phi/\partial\mathrm{X}=0$

fRe Calculation

Using the dimensionless parameter Ω then we can specify $\overline{\Omega}$ as:

$$\overline{\Omega} = -\frac{\overline{w}\mu}{H^2\left((dp/dz)+\rho_w g\right)} \tag{10}$$

Multiplying f by Re and substituting $\overline{\Omega}$, yields

$$f\mathrm{Re} = \frac{2D_h^{\,2}}{\overline{\Omega}H^2} \tag{11}$$

where $\overline{\Omega} = \iint \Omega dXdY \,/\, \iint dXdY$

The hydraulic diameter, D_h, friction factor, f, Reynolds number, Re, the average axial velocity, $\overline{w}$ are defined in the nomenclature.

Nusselt Number Calculation

The heat transfer coefficient is developed as:

$$h = \frac{q}{T_w - T_b} \tag{12}$$

where q is the average heat flux which is specified as

$$q = \frac{Q}{H + s/2} \tag{13}$$

The normalized temperature, $\overline{\theta}$, can be written as

$$\overline{\theta} = (T_w - T_b)/(Q/k) \quad \text{where} \quad \overline{\theta} = \iint \theta\Omega dXdY \,/\, \iint \Omega dXdY$$

Using the above equations, Nusselt number, Nu, can be written as

$$Nu = \frac{hH}{k} = -\frac{H}{\overline{\theta}(H + s/2)} \tag{14}$$

The present numerical technique uses the control volume method. In this method the computational domain is divided into a specified number of control volumes surrounding each grid point. The number of grids used is 20 x 50 (20 in the x-direction and 50 in the y-direction). In order to have the governing equation for each grid point, the energy and momentum equations are applied over each control volume. The resulting solution using this method implies that the integral conservation (i.e., conservation of mass, momentum and energy) is exactly satisfied for all control volumes or for the whole calculation domain shown in Figure 1. The convergence criterion was set on the values of Nu and fRe. When the difference between two consequence iterations is less than 1×10^{-6} then the iterations are stopped.

Results and Discussion

The computations were performed for grid points of 20 x 50. Larger numbers of grids were tested and similar results were achieved. A number of 140 tests were performed numerically for variable physical geometries and range of Rayleigh numbers. The normalized spacing, S, was varied from 0.1 to 1. The normalized clearance, C, was varied from 0 to 1. The Ra was varied from 0 up to 1 x 10^7.

The temperature and velocity distribution fields depend on the spacing between fins and the clearance above fin tip. The temperature distribution is shown in Figure 2. At large S the normalized temperature, θ, decreases gradually from shroud (Y=1.5) to fin base (Y=0). However, at small S the decrease in θ is sharp and the values are negligible below the fin tip. Figure 3 shows the velocity distribution. For large S, the $w/\overline{w}$ trend at low Ra tends to be parabolic, but at high Ra the $w/\overline{w}$ has negative values (reverse flow) with higher velocity in the region below the fin tip than in the region above the fin tip. For small S, the $w/\overline{w}$ is uniform below the fin tip and increases sharply above the fin tip.

The effect of changing the geometry parameters S and C, which are associated with the buoyancy force on the Nu and *f*Re at the line of symmetry, are illustrated in Figure 4. The *f*Re ratio (left vertical axis) and Nu ratio (right vertical axis) are plotted at different S value versus the clearance C above the fin tip. As shown from these figures, *f*Re and Nu ratios increase with increasing C.

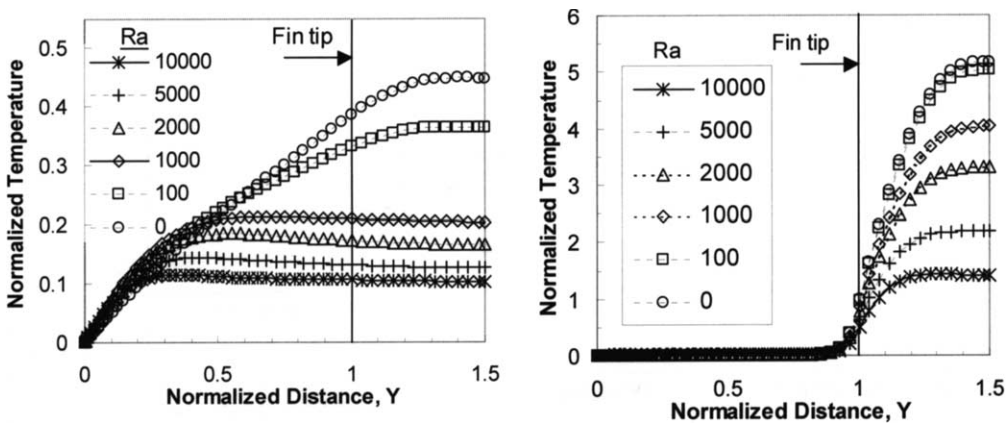

(a) (b)

FIG. 2
Normalized temperature distribution, θ, a long the line of symmetry of the fin versus normalized vertical distance at different Ra. (a) S = 1, C=0.5; (b) S=0.1, C=0.5

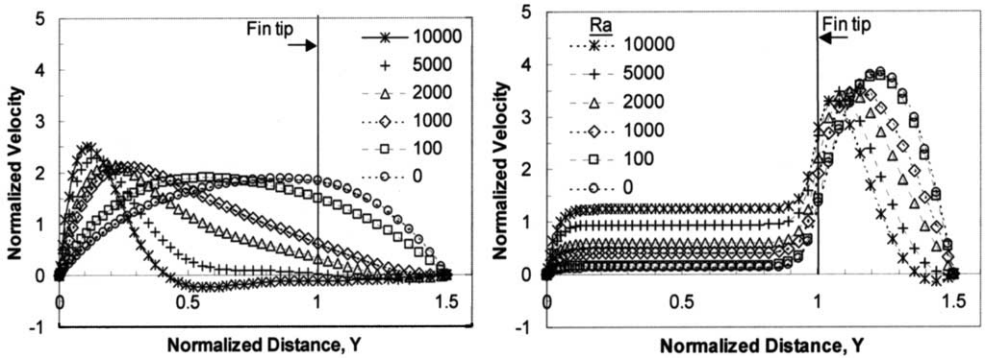

(a) (b)

FIG. 3
Normalized streamwise velocity distribution, $w/\overline{w}$, a long the line of symmetry of the fin versus normalized vertical distance at different Ra. (a) S = 1, C = 0.5; (b) S = 0.1, C = 0.5

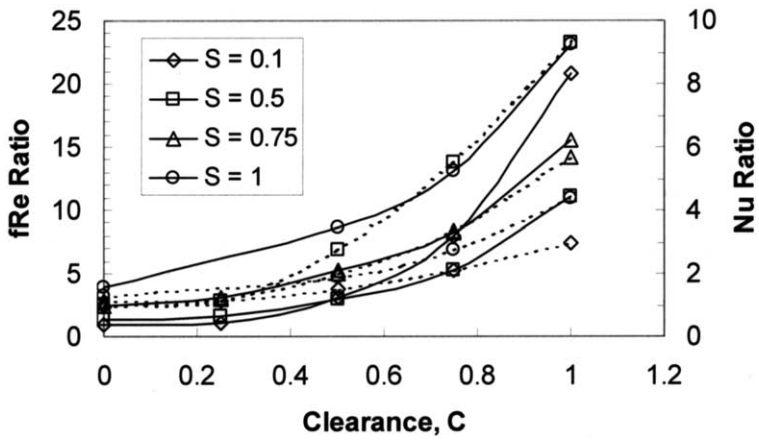

FIG. 4
Variation of Nu ratio, $(Nu)/(Nu_0)$, and f Re ratio, $(f\,\mathrm{Re})/(f\,\mathrm{Re}_0)$, with the clearance, C, above the tip of fin at Ra = 1000 (Nu ratios are in the dashed lines and *f*Re ratios are in the solid lines)

The deviation of Nu ratio and fRe from unity increases with increasing the C value. The present results agree well with those reported in ref. [11]. The buoyancy force influences the flow field distribution, which, eventually, affects the temperature distributions inside the fin. This effect can be seen clearly in Figures 5 and 6, where Nu and fRe are plotted versus Rayleigh number.

The effect of Ra on fRe and Nu is strongly dependent on the clearance above the fin tip. At no clearance the effect of Ra start after Ra = 10^6 on the contrary the effect of Ra starts at Ra around 50 for the case of C=1. Finally, three dimensional plots for the velocity and temperature distribution at small and large spacing are presented in Figures 7 to 8.

Conclusions

This work presents the characteristics performance of a vertical shrouded fin under combined free and forced convection. The velocity and temperature distributions are very sensitive to the value of Ra and geometry parameters C and S. The effect of buoyancy force demonstrated in Figures 6 and 7 by the deviations of fRe/fRe$_0$ and Nu/Nu$_0$ from unity. As the clearance, C, increases the deviation from unity starts at lower Ra and deviates sharply. The plots of the velocity distributions at the line of symmetry show reverse (i.e., negative velocity) flows at Ra greater than 5000 due to the non-uniformity of the temperature distribution caused by the buoyancy force. The spacing between the fins, S, has great influence on the velocity and temperature distribution as shown in the three-dimensional plots.

Nomenclature

c	clearance between the shroud and the tip of the fin
C	normalized clearance, c/H
C_p	specific heat of the fluid
D_h	hydraulic diameter, $(2s(H+c))/(H+s)$
f	friction factor, $-2D_h(\rho g + dp/dz)/(\rho \overline{w}^2)$
fRe	friction factor times Reynolds number
fRe$_0$	friction factor times Reynolds number at Ra =0
g	gravitational acceleration
H	fin height
h	heat transfer coefficient, q/(T_b-T_w)
k	thermal conductivity of the fluid
$\dot{m}$	mass flow rate through the array
Nu	Nusselt number, hH/k
Nu$_0$	Nusselt number at Ra = 0
p	pressure
Q	total heat input per unit axial length
q	average heat flux per unit axial length, Q/(H+s/2)
Ra	Rayleigh number

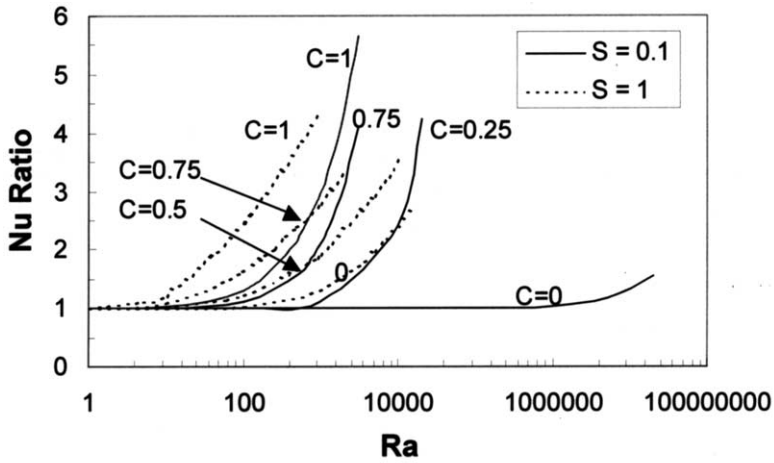

FIG. 5
Variation of $(Nu)/(Nu_0)$ with Ra

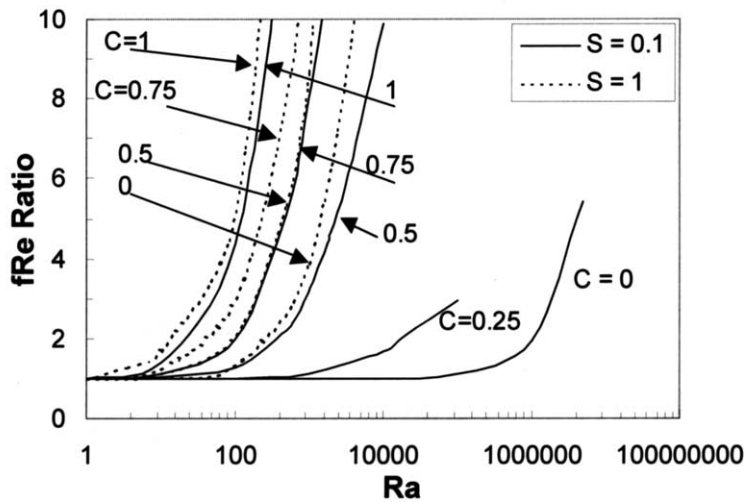

FIG. 6
Variation of $(f\,\mathrm{Re})/(f\,\mathrm{Re}_0)$ with Ra

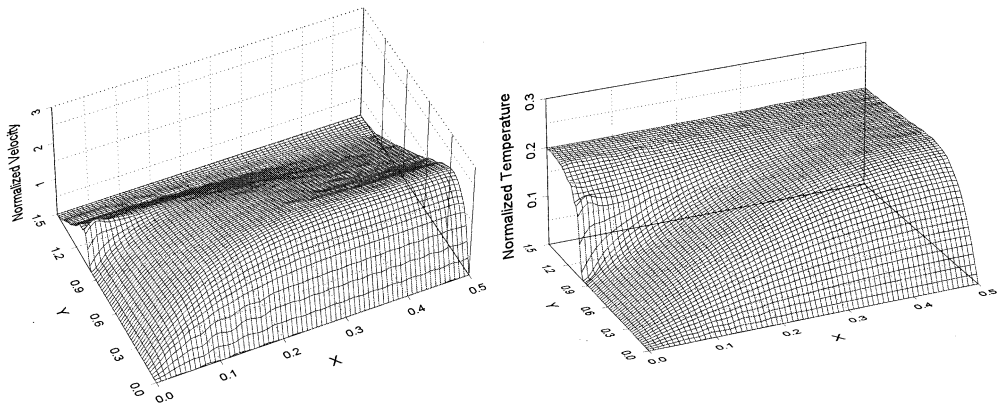

(a) (b)

FIG. 7
Normalized velocity and temperature distributions at Ra = 1000 and C = 0.5, S= 1. (a) Normalized velocity, $w/\overline{w}$; (b) Normalized temperature, θ

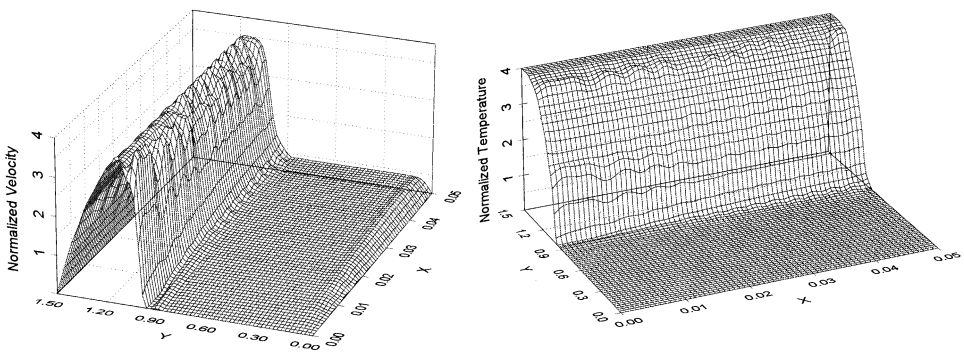

(a) (b)

FIG. 8
Normalized velocity and temperature distributions at Ra = 1000 and C = 0.5, S= 0.1. (a) Normalized velocity, $w/\overline{w}$; (b) Normalized temperature, θ

Re	Reynolds number, $(\rho \overline{w} D_h)/\mu$
s	base spacing between fins
S	normalized base spacing, s/H
T_b	bulk temperature = $\iint wTdxdy / \iint wdxdy$
T_w	wall temperature
w, $\overline{w}$	streamwise velocity, upward in the z direction, and average axial velocity, $\iint wdxdy / \iint dxdy$
x	x-coordinate w
X	normalized x coordinate, x/H
y	y-coordinate
Y	normalized y coordinate
z	streamwise upward coordinate in the flow direction
α	thermal diffusivity of the flowing fluid
β	volumetric expansion coefficient
θ	normalized temperature
μ	dynamic viscosity of the flowing fluid
ρ	density of the fluid
ρ_w	density of fluid at wall temperature
Ω	normalized axial velocity
Ω^*	the defined integral, $\iint \Omega dXdY$
ϕ	the combination, $\theta \cdot \Omega^*$

References

1. L. Jin-Sheng, L. Min-Sheng, L. Jane-Sunn, W. Chi-Chuan, *Int. J Heat Mass Transfer* **44**, 4235-4243 (2001).
2. J. Y. Yun, K. S. Lee, *Int. J Heat Mass Transfer* **42**, 2375-2385 (1999).
3. E.M. Sparrow, B.R. Baliga, S.V. Patankar , *J. Heat Transfer* **100**, 572-579 (1978).
4. E.M. Sparrow, D.S. Kadle, *J. Heat Transfer* **108**, 519-524 (1986).
5. R.A. Wirtz, W. Chen, R. Zhou, *ASME Journal of Electronic Packaging* **116**, 206-211 (1994).
6. M. Tahat, Z. H. Kodah, B. A. Jarrah, S. D. Probert, *Applied Energy* **67**,419-442 (2000).
7. O. N. Sara, T. Pekdemir, S. Yapici , M. Yilmaz, *Int. J Heat Fluid Flow* **22**, 509-518 (2001).
8. B. Watel, S. Harmand, B. Desmet, *Int. J Heat Fluid Flow* **21**, 221-227 (2000).
9. A. Daloglu, T. Ayhan, *Int. Comm. Heat Mass Transfer*, **26** (8), 1175-1182 (1999).
10. S. Acharya, S.V. Patankar, *J. Heat Transfer* **103**, 559-565 (1981).
11. Z. Zhang, S.V. Patankar, *Int. J. Heat Mass Transfer* **27**, 137-140 (1984).

Received September 13, 2002